# Exploring Serially Connected Multi-Tracked All-Terrain Vehicles for Improved Obstacle Climbing Performance

Ranjan BSC, Ujjwal Pal, Sai Prasad Ojha, Srinivasan V and Amaresh Chakrabarti*
IdeaSLab, Centre for Product Design and Manufacturing, Indian Institute of Science, Bangalore, India

* email: ac123@cpdm.iisc.ernet.in

# Exploring Serially Connected Multi-Tracked All-Terrain Vehicles for Improved Obstacle Climbing Performance

## Abstract

The paper presents design specification of three tracked all-terrain vehicles: a 'Single Tracked Vehicle' (STV), where the payload is placed between two single, parallel tracks, a 'Double Tracked Vehicle' (DTV) where two sets of two serially connected tracks are joined together, and a 'Triple Tracked Vehicle' (TTV) where two sets of three serially connected tracks are joined together in parallel to carry the load. The paper provides a theoretical model for the obstacle climbing ability of the vehicles, where an obstacle is defined as a step. A model of each vehicle is developed using Lego-Mindstorms™ toolkit, and experiments are conducted to find the maximum heights and the maximum slopes climbed by each vehicle. It is found that the TTV has a substantially better obstacle climbing ability than Shrimp III – the existing robot with the best climbing performance. The results compare well with the theoretical models.

**Keywords:** all-terrain vehicle, tracked vehicle, obstacle climbing performance, serially multi-tracked vehicle

## 1 Introduction

The term "All-Terrain Vehicle" or ATV is used in a general sense to describe any of a number of small open motorized buggies and tricycles designed for off-road use. As the name suggests, these vehicles are designed to handle a wider range of terrains than conventional vehicles. Obstacle navigation is one of the essential functionalities that must be considered while designing an ATV. An ATV during its navigation is expected to encounter obstacles of all shapes and sizes. There have been many efforts in the past to design vehicles that can overcome different kinds of obstacles. Vehicle locomotion in rough terrain is a holistic problem. Navigation in rough terrains is a fast evolving field of research. During navigation, the vehicles should be able to tackle the obstacles in their path and climb different kinds of terrain. The objective of this paper is to develop a mobility platform for an all-terrain vehicle which can negotiate large slopes and obstacles. The particular focus of this paper is on developing *tracked vehicles* that can climb greater slopes and heights.

A slope is specified as the degree of inclination of a terrain to the horizontal plane. An obstacle is taken here as a step with a slope of 90 degrees.

The paper is structured as follows: Section 2 provides an overview of literature on existing vehicles and their capabilities, Section 3 describes the design specifications of the single-, double- and Triple Tracked Vehicles developed as part of this research; Section 4 reports results from physical tests and analytical models of these vehicles; Section 5 discusses results of comparison of the vehicles developed in this work with the best available vehicle; and Section 6 provides conclusions.

## 2 Literature Survey

While a great deal of prior mobile robot research is available, the vast majority has either used wheeled vehicles or worked primarily with a large number of actuators. There are many configurations in which a mobile robot can be made. If the robot has to move only on a flat terrain, conventional wheels are sufficient, however, if the robot has to move on a staircase or an uneven terrain, a special system may be required.

Robot mobility systems can be divided into wheeled, tracked, legged or hybrid systems. A review of existing work follows. The Neptune robot [1] is a three-tracked magnetic rover built for the inspection of the oil tankers and can climb to any height of magnetic surface inside the tanker. It fits into a 20 inch diameter tube. It consists of six separate entities: the robot crawler with its magnetic tracks, the on-board vision and ultrasonic sensor, the onboard control and telemetry system, the on-board and in-tank navigation system, the deployment system atop the tank, the remote operator console and the display and control software. The ROBHAZ-DT [2] with a size of 484 mm x 319 mm x 720 mm and a mass of 50 kg (including batteries) is a variable double-tracked mobile robot used in environment hazardous to human health. It can negotiate a maximum step angle of 40 degrees. This robot consists of four tracks and powered by four motors. The two tracks are connected with the help of a wheel. The controllers and motors are attached in the mid-segment of the vehicle. In the front, the power control system is fixed with an emergency switch, which can turn on or off the power with a current sensor and RF remote controller to prevent an overload. The modified version of ROBHAZ-DT is ROBHAZ-DT3 [3] with a mass of 39 kg (including batteries) and a size of 740 mm x 470 mm x 290 mm. It can negotiate a maximum slope of 40 degrees. The Securities [4], a four-tracked vehicle with a mass of 1000 kg is able to negotiate a maximum slope of 45 degrees and a maxi-

mum height of 230 mm. The robot is autonomous and is powered using a set of batteries. The maximum speed is about 0.3 m/s; the speed reduction is obtained by cycloidal reducers and toothed belt drivers tensioned by eccentric pulleys. The Urban-II [5] with a mass of 20 kg (including batteries) can climb a maximum height of 20 cm. The PACKBOT [6] is a tracked robot with a small main chassis profile and has a height of 20.32 cm. It can negotiate a maximum slope of 60 degrees. The Transformable Crawler [7], a tracked vehicle has a pair of tracks fitted on two sides of its body. The drive wheels are driven by the drive units, which consist of a DC motor, reduction gear, negative brake and rotation sensor. The overall size of the robot is 87.5 cm x 166 cm x 30.5 cm. It has a load mass of 105 kg and tare mass of 175 kg and can climb 203 mm and 39.3 degrees of slope. Shrimp III [8] is a wheeled vehicle with a wheel diameter of 11.6 cm and is able to climb a step of 22 cm height. It is biologically inspired by the sea creature "shrimp". Shrimp III rover has six wheels that operate separately; back and front wheels and four side wheels that are mounted in parallel bogies system, and the front wheel is placed on a front-fork mechanism. MFEX [9] is another wheeled vehicle with a wheel diameter of 130 mm and can climb a step height of 180 mm. Marsokhod [9], a vehicle that uses wheels for locomotion has a wheel diameter of 350 mm, can climb a step of 500 mm height. The Millibot [10] is a series of wheeled robots linked together to negotiate difficult terrains, like a flight of stairs. Rocky 7 [11] employs a rocker bogie six wheel configuration and has steering capabilities on two corners of its wheels. The step climbing ability is approximately 1.5 times its wheel diameter. The Rocky 7 is located midway between the double wheel pairs. The dimensions of the Rocky 7 are 610 x 490 x 310 mm. The wheel diameter is 130 mm. The maximum speed on a normal flat ground is 30 cm/s. Work Partner [12] is a multitasked outdoor robot. It's targeted for light outdoor applications like property maintenance, gardening and light forestry tasks. The hybrid locomotion system provides four motorized wheels with articulated steering for easy terrain. Four legs, each having three degrees of freedom make it possible to perform walking and control the body attitude with ease. The total weight of Work partner is about 230 kg, the payload is about 50 kg and it can handle objects up to 10 kg. The hybrid energy system is based on small batteries (48V) and a supporting unit, which can be either 1 kW motor - generator or 500W alkali fuel cell. All actuators are electric. Hylos [13] is a high mobility redundantly actuated vehicle. It is a lightweight mini-robot with 16 actively actuated degrees of freedom (four wheel-legs, each one combining two degrees of freedom suspension mechanism with a steering and driven wheel). The actuated degrees of freedom of this robot are split in two categories: the first one concerns the locomotion itself (traction and steering) and the second one the posture (orientation of the main body and sideway wheelbases). The Hylos wheel-legged robot is approximately 60 cm long and weighs 12 kg. It climbs a slope of 38 degrees. Chugo et al. [14] have developed a prototype that uses seven free rolling wheels and passive links. Its 12 cylindrical rollers apply traction only in one direction of travel. Its wheels are actuated and generate omni directional movement through a suitable wheel arrangement and control. The vehicle can negotiate a step of 152 mm step using a wheel of 132 mm diameter. Micro5 [15] is a Japanese five wheeled lunar rover. It uses suspension system named Pegasus [16]; uses a fifth wheel to support the remaining wheels while front wheels climb obstacles. The rover with 100 mm wheel diameter is able to climb a 150 mm high step. Pegasus mobility system has 4 active wheels and one extra wheel which are connected to the body with an actuated joint. When front wheels climb, the fifth wheel carries some part of the weight to provide better stability for the vehicle and help climb the obstacle.

In order to normalize our findings for purposes of comparison, we have developed two measures: (a) Ratio of maximum height of obstacle climbed ($H_{ob}$) to wheel diameter ($d_{wh}$) and (b) Ratio of maximum obstacle height climbed ($H_{ob}$) to vehicle height (H). Table 1 summarizes our findings of the existing vehicles from a perspective of their ability to climb. Measure (a) is useful particularly for comparison of wheeled vehicles of various wheel sizes. Measure (b) is proposed to provide a comparison of both non-wheeled and wheeled vehicles, to provide an estimate of the relative height of payload climbed against the height of obstacle climbed.

It was found that none of the vehicles [1, 4-6, 10, 12-16] were able to cover an obstacle height more than twice that of its wheel diameter or track height. A survey of literature revealed a number of vehicles that are claimed to climb great heights but these could not be included in this paper because quantitative data required for the comparison are not given. Among those for which relevant quantitative data is available, (Table 1) Shrimp III [8] has the best step-climbing performance.

**Table-1:** Existing robots and their climbing abilities

| **Vehicle** | **LxWxH (mm)** | **$d_{wh}$ (mm)** | **$H_{ob}$ (mm)** | **$H_{ob}$/ $d_{wh}$** | **$H_{ob}$/ H** |
|---|---|---|---|---|---|
| ROBHAZ-DT [2] | 720x484x 319 | ~ 200 | 180 | 0.9 | 0.56 |
| ROBHAZ-DT3 [3] | 290x470x 740 | ~ 200 | 180 | 0.9 | 0.24 |
| Trans-formable Crawler [7] | 1600x874x 305 | 305 | 203 | 0.66 | 0.66 |
| **Shrimp III [8]** | **639x429x 228** | **116** | **220** | **1.89** | **0.96** |
| MFEX [9] | 630x480x 280 | 130 | 180 | 1.38 | 0.64 |
| Marsokhod [9] | 1200x950x 1000 | 350 | 500 | 1.42 | 0.5 |
| Rocky 7 [11] | 610x490x 310 | 130 | 195 | 1.5 | 0.63 |

# 3 Results

Tracked vehicles run with the help of tracks. This class

of vehicles has a larger surface area of contact with the ground, thereby enabling them to distribute their weight over a larger area. This is particularly helpful while navigating in soft, low friction and uneven terrains. This class of vehicles also offer greater stability owing to better load distribution in uneven and rough terrains. Since the broad objective of this paper is to develop a mobility system for an all-terrain vehicle especially during obstacle navigation, we focus our efforts on tracked systems for the advantages they offer. STVs have often been explored in literature. On the other hand, vehicles with two and three serially connected tracks have not been experimented with before. In this paper, we have developed vehicles with two parallel track chains, where each chain contains one, two or three tracks that are serially connected with each other using hinged joints. A physical model for each of these vehicles has been developed using Lego-Mindstorms ™ toolkit.

### 3.1 Single Tracked Vehicle

The physical model of the STV developed is shown in Figure 1. The track height (including the diameter of the wheel driving the track) is 29 mm. The vehicle is run with the help of one RCX and four motors. The RCX is powered by 6 AA Ni-Cd batteries, each of 1.5V. The vehicle is able to climb a maximum step height of 22 mm. The other specifications of the STV model are given in Table 2.

### 3.2 Double Tracked Vehicle

The physical model for the DTV developed is shown in Figure 2. The track height (including the diameter of the wheel driving the track) is 29 mm. The vehicle is run with the help of one RCX and four motors. The RCX is powered by 6 AA Ni-Cd batteries, each of 1.5V. The two tracks are serially connected with a hinge joint, whose movement is limited with the use of flexible, inextensible members that act as mechanical 'limit switches', flexible, members, in order to avoid folding of the tracks on each other. The vehicle is able to climb a maximum step height of 41 mm. The other specifications of the DTV model are given in Table 2.

### 3.3 Triple Tracked Vehicle

The TTV is shown in Figure 3. The track height (including the diameter of the wheel driving the track) is 29 mm. The vehicle is run with the help of one RCX and four motors. The RCX is powered by 6 AA Ni-Cd batteries, each of 1.5V. To create the TTV, the double tracks of the DTV are serially connected with another track using a hinge joint, whose movement is limited using flexible, inextensible members, to avoid folding of the tracks on one another other. The vehicle is able to climb a maximum step height of 84 mm – almost three times its track height. The other specifications of the TTV model are given in Table 2.

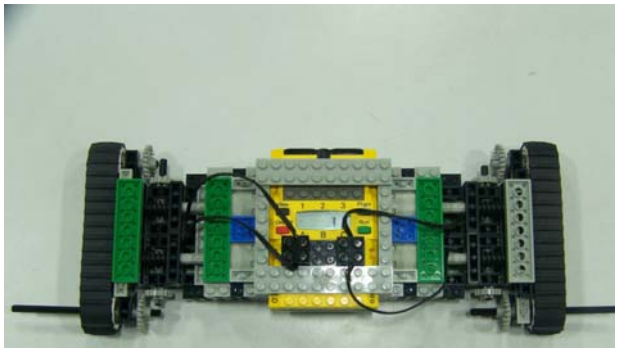

Fig.1: A model of the STV

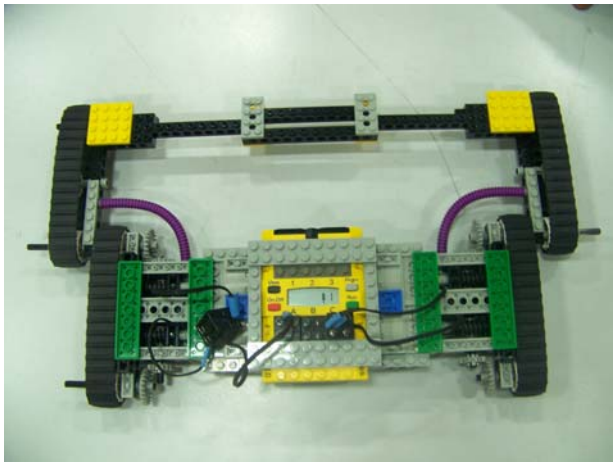

Fig. 2: A model of the DTV.

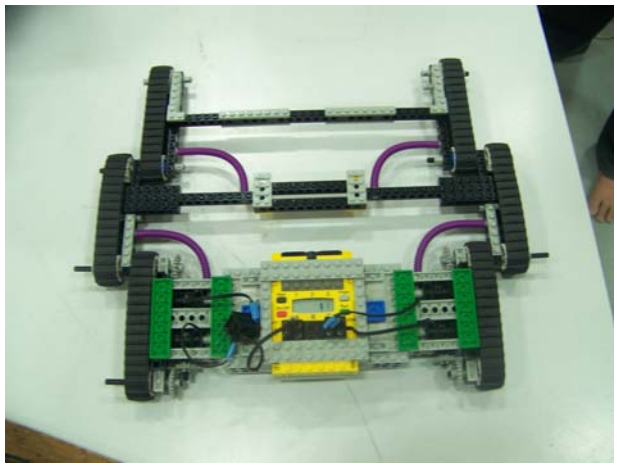

Fig. 3: A model of the TTV

**Table-2:** Specifications of STV, DTV and TTV

| Vehicle type | L x W x H (mm) | Mass (kg) | Track width (mm) | Velocity (mm/s) |
|---|---|---|---|---|
| STV | 299x126x58 | 0.667 | 20 | 13.66 |
| DTV | 360x222x58 | 0.76 | 20 | 13.21 |
| TTV | 360x318x58 | 0.849 | 20 | 12.5 |

## 4 Analysis

The step climbing performance of each of the three

tracked vehicle models is assessed analytically using force and moment balance equations as well as geometric constraints.

## 4.1 Single-tracked vehicle (STV)

The free body diagram (FBD) of the STV is given in Fig. 4, where the track is shown trying to climb a step of height h. Refer Table 3 for a description of symbols.

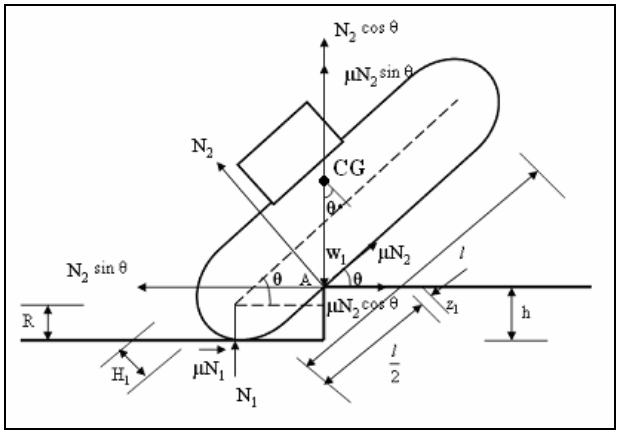


Fig. 4: FBD of a STV climbing a step

Considering force balance in vertical direction,

$$N_1 + N_2 \cos\theta + \mu N_2 \sin\theta = W_1 \quad (1)$$

Considering force balance in horizontal direction,

$$\mu N_1 + \mu N_2 \cos\theta = N_2 \sin\theta \quad (2)$$

The STV will climb the step, if the clockwise moment about A is greater than the anti-clockwise moment, i.e.,

$$\mu N_1 h \le N_1\left[\left(l/2 + z_1\right)\cos\theta + H_1 \sin\theta\right]$$

which can be reduced to

$$h \le \left(\frac{1}{\mu}\right)\left[\left(l/2 + z_1\right)\cos\theta + H_1 \sin\theta\right] \quad (3)$$

From geometry one could derive this constraint:

$$h = H_1\cos\theta + (\frac{l}{2} + z_1)\sin\theta + R - (\frac{H_1}{\cos\theta} + \frac{R}{\cos\theta}) \quad (4)$$

**Table-3:** Symbols and their descriptions for STV

| Symbol | Description |
|---|---|
| CG | Centre of gravity of the vehicle |
| $W_1$ | Weight of the vehicle |
| $N_1$, $N_2$ | Normal reaction force |
| μ | Co-efficient of friction |
| θ | Angle between the track and the horizontal |
| 2R | Height of the track |
| l+2R | Length of the track |
| $z_1$ | Distance of CG from geometric centre of the track measured parallel to its axis |
| $H_1$ | Distance of CG from geometric centre of the track measured perpendicular to its axis |
| h | Height of step |

To climb the step shown in Figure 4, the above equations have to be satisfied. The maximum height of the step that the vehicle can climb is the maximum value of h obtained from Eq. (4) for $0 \le \theta \le 90°$, that satisfies the other three equations. The values of the parameters, as estimated from the physical model, are given in Table 6. Solving using the above procedure we obtain the maximum value of 'h' as 22.74 mm. Tests using the physical model of the STV model revealed that the vehicle was able to climb a maximum height of 22 mm.

## 4.2 Double-tracked vehicle (DTV)

The free body diagram of the DTV is shown in Figure 5. Refer Table 4 for a description of symbols.

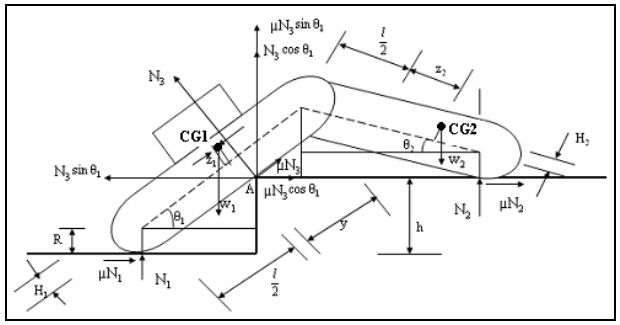


Fig 5: Free body diagram of DTV climbing a step

**Table-4:** Symbols and their descriptions for DTV

| Symbol | Description |
|---|---|
| CG1, CG2 | CG of the rear and front segments |
| $W_1$, $W_2$ | Weight of the rear and front segments |
| $N_1$,$N_2$,$N_3$ | Normal reaction forces |
| μ | Co-efficient of friction |
| $\theta_1$, $\theta_2$ | Angle between the rear and front tracks and the horizontal |
| 2R | Height of the track |
| l+2R | Length of the track |
| $z_1$, $z_2$ | Distance of CG from geometric centre of the rear and front tracks measured parallel to their respective longitudinal axis |
| $H_1$, $H_2$ | Distance of CG from geometric centre of the rear and front tracks measured perpendicular to their respective longitudinal axis |
| h | Height of step |

Considering force balance in vertical direction,

$$\sum V \rightarrow N_1 + N_2 + N_3 Cos\theta_1 + \mu N_3 Sin\theta_1 = W_1 + W_2 \quad (5)$$

Considering force balance in horizontal direction,

$$\sum H \rightarrow \mu N_1 + \mu N_2 + \mu N_3 Cos\theta_1 = N_3 Sin\theta_1 \quad (6)$$

The DTV will climb the step, if the clockwise moment about A is greater than the anti-clockwise moment, i.e.,

$$[(l-y)Cos\theta_1 + RSin\theta_1]N_1 + [(\frac{l}{2} + z_2)Cos\theta_2 + (yCos\theta_1 - RSin\theta_1) + H_2 Sin\theta_2]W_2 \ge \mu N_1 h + [(\frac{l}{2} - z_1 - y)Cos\theta_1 + (H_1 + R)Sin\theta_1]W1 + [lCos\theta_2 + yCos\theta_1 - RSin\theta_1]N_2 \quad (7)$$

From geometry one could derive the following:

$$y = l - \frac{h}{Sin\theta_1} + \frac{R}{Sin\theta_1}(1 - Cos\theta_1) \quad (8)$$

When the vehicle just starts to climb the step, the contact between the rear track and ground is lost and $N_1$ becomes zero. Solving for $N_2$ and $N_3$ from Eq. (5) and (6):

$$N_2 = \frac{(Sin\theta_1 - \mu Cos\theta_1)(W_1 + W_2)}{(1 + \mu^2)Sin\theta_1}$$

$$N_3 = \frac{\mu(W_1 + W_2)}{(1 + \mu^2)Sin\theta_1}$$

From geometry one could derive that,

$$Sin\theta_2 = Sin\theta_1 - \frac{h}{l} \quad (9)$$

Substituting $N_2$, $N_3$ and y (from Eq. (8)) in Eq. (7) we get an expression as a function of variables – $\theta_1$, $\theta_2$ and h, and constants – $W_1$, $W_2$, $z_1$, $z_2$, $H_1$, $H_2$, l, μ and R. This expression and Eq. (9) give the necessary conditions for the DTV to climb the step. The maximum step height that the DTV can climb is the maximum value of h obtained from Eq. (9) for $0 \le \theta_1, \theta_2 \le 90°$, that satisfies Eq. (7) after substituting $N_2$, $N_3$ and y. The values of the constants used, as estimated from the physical model, are given in Table 6. Solving using the above procedure, the maximum value of h obtained is 41.75 mm. Test runs of the physical model of the DTV revealed that the vehicle was able to climb a maximum height of 41 mm.

## 4.3 Triple Tracked Vehicle (TTV)

The free body diagram of the TTV is shown in Figure 6. Refer Table 5 for a description of symbols. Considering force balance in vertical direction,

$$\sum V \rightarrow N_1 + N_2 + N_3 Cos\theta_1 + \mu N3 Sin\theta_1 + N_4 = W_1 + W_2 + W3 \quad (10)$$

Considering force balance in horizontal direction,

$$\sum H \rightarrow \mu N_1 + \mu N_2 + \mu N_4 + \mu N_3 Cos\theta_1 = N_3 Sin\theta_1 \quad (11)$$

The TTV will climb the step, if the clockwise moment about A is greater than the anti-clockwise moment, i.e.,

$$[(\frac{l}{2} + z_2)Cos\theta_2 + H_2 Sin\theta_2 + yCos\theta_1 - RSin\theta_1]W_2 +$$

$$[(\frac{l}{2} + z_3) + (lCos\theta_2 + yCos\theta_1 - RSin\theta_1)]W_3 \ge$$

$$[(\frac{l}{2} - z_1 - y)Cos\theta_1 + (H_1 + R)Sin\theta_1]W_1 \quad (12)$$

$$+[lCos\theta_2 + yCos\theta_1 - RSin\theta_1]N_2$$

$$+[(\frac{l}{2} + z_3) + (lCos\theta_2 + yCos\theta_1 - RSin\theta_1)]N_4$$

From geometry one could derive that,

$$y = l - \frac{h}{Sin\theta_1} + \frac{R}{Sin\theta_1}(1 - Cos\theta_1) \quad (13)$$

$$Sin\theta_2 = Sin\theta_1 - \frac{h}{l} \quad (14)$$

When the vehicle just starts to climb the step, the contact between the rear track and ground is lost and $N_1$ becomes zero. Solving for $N_2$, $N_3$ and $N_4$ from Eq. (10)-(12) and substituting $N_2$, $N_4$ and y (from Eq. (13)) in Eq. (12) we get an equation involving variables - $\theta_1$, $\theta_2$ and h, and constants – $W_1$, $W_2$, $W_3$, $z_1$, $z_2$, $z_3$, $H_1$, $H_2$, l, μ and R. This equation and Eq. (14) give the necessary conditions for the TTV to climb the step. The maximum height of the step that the vehicle can climb is the maximum value obtained from Eq. (14) for $0 \le \theta_1, \theta_2 \le 90°$, that satisfies Eq. (12) after substituting $N_2$, $N_4$ and y. The values of constants (parameters), as estimated from the physical model, are given in Table 6. Solving using the above procedure, we obtain the maximum value of 'h' as 95.6 mm. Test runs performed using the physical model of the TTV developed showed that the vehicle was able to climb a maximum height of 84 mm.

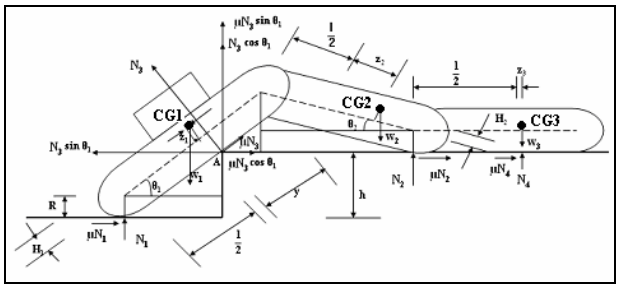


Fig 6: FBD of TTV climbing a step

**Table-5:** Symbols and their descriptions for TTV

| Symbol | Description |
|---|---|
| CG1, CG2, CG3 | Centre of gravity of rear, middle and front tracks |
| $W_1, W_2, W_3$ | Weight of the rear, middle and front portions of the vehicle |
| $N_1, N_2, N_3, N_4$ | Normal reaction forces |
| μ | Co-efficient of friction |
| $\theta_1$, $\theta_2$ | Angle between the rear and middle tracks, and the horizontal |
| 2R | Height of the track |
| l+2R | Length of the track |
| $z_1$, $z_2$, $z_3$ | Distance of CG from geometric centre of the rear, middle and front tracks measured parallel to respective longitudinal axis |
| $H_1$, $H_2$ | Distance of CG from geometric centre of the rear and middle tracks measured perpendicular to respective longitudinal axis |
| h | Height of step |

**Table-6:** Parameters for STV, DTV and TTV

| Parameter | STV | DTV | TTV |
|---|---|---|---|
| l (mm) | 96 | 96 | 96 |
| R (mm) | 14.5 | 14.5 | 14.5 |
| $H_1$ (mm) | 6.48 | 6.48 | 6.48 |
| $H_2$ (mm) | N/A | 3.57 | 3.57 |
| $z_1$ (mm) | 0.3 | 0.3 | 0.3 |
| $z_2$ (mm) | N/A | 12.38 | 12.38 |
| $z_3$ (mm) | N/A | N/A | 1.4 |
| $W_1$ (kg) | 0.667 | 0.667 | 0.667 |
| $W_2$ (kg) | N/A | 0.0956 | 0.0956 |
| $W_3$ (kg) | N/A | N/A | 0.086 |
| μ | 0.8 | 0.8 | 0.8 |

## 4.4 Toppling condition for STV

Considering force balance in vertical and horizontal directions (Figure 7),

$$N_1 = W_1 \cos\theta \quad (15)$$

$$\mu N_1 = W_1 \sin\theta \quad (16)$$

If the STV has to topple, then anti clockwise moment about A should be greater than clockwise moment about A.

$$W_1(H_1 + R)\sin\theta \geq (\frac{l}{2} + z_1)N_1$$

$$\text{or } \tan\theta \geq \frac{\frac{l}{2} + z_1}{H_1 + R} \quad (17)$$

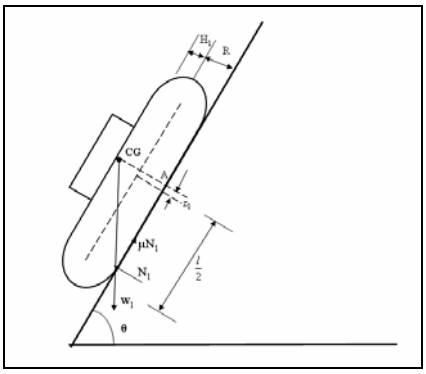


Fig 7: FBD of STV climbing slope

Solving using the data from Table 6 we obtain the minimum value of θ as 70.4º which is greater than the friction angle. So it will not topple during climbing of slope 33.2º. Tests using the physical model of the STV revealed that the vehicle was toppled at an angle of 68º.

## 4.5 Toppling condition for DTV

Considering the force balance of rear track (Figure 8),

$$W_1 cos\theta + Y = N_1 \quad (18)$$

$$W_1 sin\theta + X = \mu N_1 \quad (19)$$

Taking moment about point A,

$$XR = Yl \quad (20)$$

Considering the force balance of front track,

$$N_2 = W_2 cos\theta + Y \quad (21)$$

$$X + \mu N_2 = W_2 sin\theta \quad (22)$$

Taking moment about point C,

$$\mu N_2 R + N_2[(\frac{l}{2} + z_2) - H_2 \tan\theta - R\tan\theta] = [(\frac{l}{2} + z_2)cos\theta - H_2 sin\theta]W_2 \quad (23)$$

When the vehicle just starts to topple, anti clockwise moment about A should be greater than clockwise moment about A for the rear track and clockwise moment about C should be greater than clockwise moment about C for the front track as the CG of rear track is much higher than the CG of front track from the center line. So the toppling conditions are

$$XR \geq Yl \quad (24)$$

$$[(\frac{l}{2} + z_2)cos\theta - H_2 sin\theta]W_2 \geq \mu N_2 R + N_2[(\frac{l}{2} + z_2) - H_2 \tan\theta - R\tan\theta] \quad (25)$$

Solving for $N_1$, N2, X and Y from Eq. (18)-(19) and Eq. (21)-(22) and substituting X and Y in Eq. (24) and $N_2$ in Eq. (25) and varying θ from 0 to 90º, we get a minimum θ that satisfy Eq. (24) and (25). Solving using the above procedure we obtain the minimum value of 'θ' as 79º which is greater than the friction angle. So it will not topple during climbing of slope 33.2º. Tests using the physical model of the DTV revealed that the vehicle was toppled at an angle of 73.4º.

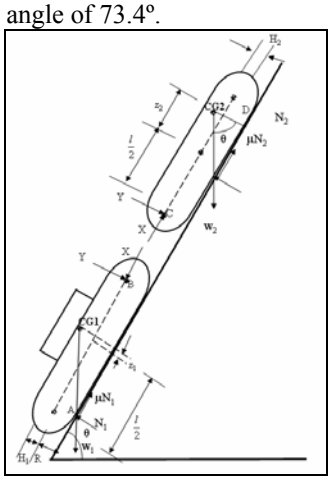


Fig 8: FBD of DTV climbing slope

## 4.6 Toppling condition for TTV

Considering the force balance of rear track (Figure 9),

$$W_1 cos\theta + Y_1 = N_1 \quad (26)$$

$$W_1 sin\theta + X_1 = \mu N_1 \quad (27)$$

Taking moment about point A,

$$X_1 R = Y_1 l \quad (28)$$

Considering the force balance of middle track,

$$N_2 = W_2 cos\theta + Y_2 + Y_1 \quad (29)$$

$$X_1 + \mu N_2 = W_2 sin\theta + X_2 \quad (30)$$

Taking moment about point C,

$$\mu N_2 R + N_2 l + X_2 R = [(\frac{l}{2} + z_2)cos\theta - H_2 sin\theta]W_2 + Y_2 l \quad (31)$$

Considering the force balance of front track,

$$N_3 = W_3 cos\theta + Y_2 \quad (32)$$

$$X_2 + \mu N_3 = W_3 sin\theta \quad (33)$$

Taking moment about point E,

$$[(\frac{l}{2} + z_3)cos\theta - H_3 sin\theta]W_3 = \mu N_3 R + [(\frac{l}{2} + z_3) - H_3 tan\theta - R\tan\theta]N_3 \quad (34)$$

When the vehicle just starts to topple, clockwise moment about C should be greater than clockwise moment about C for the middle track and clockwise moment about E should be greater than clockwise moment about E for the front track. So the toppling conditions are

$$\mu N_2 R + N_2[(\frac{l}{2} + z_2) - H_2 \tan\theta - R\tan\theta] + X_2 R \geq [(\frac{l}{2} + z_2)cos\theta - H_2 sin\theta]W_2 + Y_2 l \quad (35)$$

and

$$[(\frac{l}{2} + z_3)cos\theta - H_3 sin\theta]W_3 = \mu N_3 R + [(\frac{l}{2} + z_3) - H_3 tan\theta - R\tan\theta]N_3 \quad (36)$$

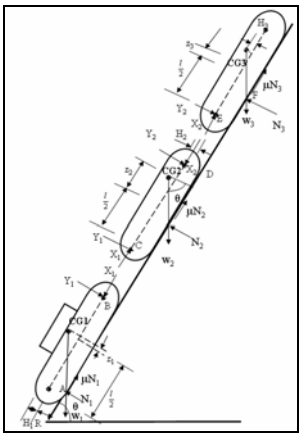

Fig 9: FBD of TTV climbing slope

Solving for $N_1$, $N_2$, $N_3$, $X_1$ , $Y_1$ ,$X_2$ and $Y_2$ from Eq. (26)-(30) and Eq. (32)-(33) and substituting $X_2$ ,$Y_2$ , $N_2$ and $N_3$ in Eq. (34) and (35) and varying θ from 0 to 90º, we get a minimum θ that satisfy Eq. (35) and Eq. (36). Solving using the above procedure we obtain the minimum value of 'θ' as 77º which is greater than the friction angle. So it will not topple during climbing of slope 34.1º. Tests using the physical model of the TTV revealed that the vehicle was toppled at an angle of 70.6º.

**Table-7**: Toppling & friction angles for the vehicles

| Vehicle | STV | DTV | TTV |
|---|---|---|---|
| Theoretical toppling angle (deg) | 70.4 | 79 | 77 |
| Experimental toppling angle (deg) | 68 | 73.4 | 70.6 |
| Friction angle (deg) | 35.6 | 35.6 | 35.6 |

Table 7 provides an overview of the minimum angles for toppling from analytical models and physical tests, both showing a similar trend. In is interesting to note that the minimum angle is maximum for the DTV, followed by that for the TTV, with STV being the most prone to toppling. Experimental results give lower values than those obtained from the analytical models. This could be due to the somewhat different operating condition used in the physical tests (to avoid sliding, slope is changed keeping the vehicle stationary on the slope rather than making it climb the slope). The better performance of the DTV may be due to the stabilizing effect of its front track on its rear track, as opposed to none in the case of the STV, and as opposed to the destabilizing effect of the front track on the middle track enhancing the tendency of toppling of its rear track in the case of TTV.

# 5 Comparison

Height climbing ability of the three tracked vehicles and the Shrimp III – the existing robot with the best step climbing performance – are given in Table 8. Also shown, for the tracked vehicles, are the maximum heights theoretically possible to climb by each vehicle, as found from the analyses detailed earlier in the paper.
As can be seen from the table, the performance of the tracked vehicles improve consistently as the number of serial tracks increase, with the TTV giving the best performance. The values of the maximum height calculated theoretically match closely with the actual values for the first two cases, while in the case of the TTV it does not match well the theoretical maximum estimated for the TTV, although it does not violate the theoretical maximum obtained. Possible reasons for this are as follows:

- Considerable slippage occurs between the gears used, which contributes to loss of traction, particularly at the near-90 degree climb for the rear track while trying to climb a height close to its length.
- The mechanics of climb may be somewhat different from what is used in the theoretical analysis (where the first track is flat on the ground). Due to use of shorter span step, this is not always achieved.
- The mechanics of climb is also variable due to the two tracks not necessarily climbing the step at the same time, giving various angles, both vertical and horizontal, at which the climb is approached.
- The motors may not be powerful enough to provide the maximum traction assumed in analytical models.

As detailed earlier in the paper, two normalized criteria are used for comparing performance of vehicles of various sizes climbing various step heights:

- Maximizing the ratio of obstacle height to wheel diameter (or track height for tracked vehicles);
- Maximizing the ratio of obstacle height to vehicle height (this is to check the ability of a vehicle to allow maximum possible space for its payload).

Using either of the criteria, the TTV seems to perform substantially better than all the vehicles reported in literature, climbing about three times its track height compared to less than twice as achieved by Shrimp III (the vehicle among those reported in literature with the best step climbing performance), as well as having a much better obstacle height to vehicle height ratio. Even DTV performs as well as Shrimp III against this latter criterion, although not as well against the former criterion.

**Table-8:** Comparison of performance of vehicles

| **Vehicle** | **$H_{ob}$ (mm)** | **$H_{ob}/d_{wh}$** | **$H_{ob}/H$** | **Theoretical $H_{ob}$ (mm)** |
|---|---|---|---|---|
| STV | 22 | 0.76 | 0.38 | 23.16 |
| DTV | 41 | 1.41 | 0.71 | 41.75 |
| TTV | 84 | 2.90 | 1.45 | 95.60 |
| Shrimp-III | 220 | 1.89 | 0.96 | Not known |

In addition, tests using the models have shown that these

tracked vehicles have an attractive slope climbing ability (Table 9). These vehicle models have been tested at various slopes with a limiting coefficient of friction of 0.71 (friction angle of 35.6 degrees); the corresponding maximum slopes climbed were 32-34 degrees. The maximum slope climbed by the three vehicle types is fairly similar. It is not clear why the TTV performs slightly better in slope climbing that the other two variants. This is possibly due to its better distribution of weight over a larger area, taking advantage of a wider variety of different friction coefficients as typically found in realistic terrains, thereby reducing the chance of its performance getting much affected by local variations in the friction characteristics of the surface climbed.

**Table-9:** Comparison of slope-climb performance

| **Vehicle** | **Max slope climbed (degrees)** | **Angle of limiting sliding friction (deg)** |
|---|---|---|
| Single-tracked | 33.2 | 35.6 |
| Double-tracked | 33.2 | 35.6 |
| Triple-tracked | 34.1 | 35.6 |

# 6 Conclusions

This class of tracked vehicles (with multiple serially connected tracks) seems to have a high obstacle climbing ability. They also have a good slope climbing ability.

# Acknowledgment

We thank ISRO for funding an earlier project related to design of mobility systems of all-terrain vehicles which motivated us to develop the reported class of vehicles.

# References

[1] H. Schempf, B. Chemel and N. Everett, "Neptune: Above-Ground Storage Tank Inspection Robot System," *IEEE Robotics & Automation Magazine*, June, 1995, pp. 9-15.

[2] C. Cho., C. Park., S. Kang., M. Kim., C. Lee. and Y. K. Kwak., "ROBHAZ-DT: Variable Configuration Double-Track Mobile Robot for Hazardous Environment Applications", *Proc. of International.Conference on Control, Automation and Systems (ICCAS2001), pp.150-153, Cheju, 2001.*

[3] W. Lee, S. Kang, M. Kim and M. Park, "ROBHAZ-DT3 Teleoperated Mobile Platform with Passively Adaptive Double-Track for Hazardous Environment Applications", *Proc. of International Conference on Intelligent Robots and Systems (IROS 2004), Vol. 1, pp. 33-38, Sendal, 2004.*

[4] A. Romiti and T. Raparelli, "Four Track Mobile Robot for Non-Structured Environments," *Proc. Of International Conference on Advanced Robotics (ICAR91), Vol. 2, pp. 926-930, Pisa, 1991.*

[5] L. Matthies, Y. Xiong, R. Hogg, D. Zhu, A. Rankin, B. Kennedy, M. Hebert, R. Maclachlan, C. Won, T. Frost, G. Sukhatme, M. McHenry and S. Goldberg, "A Portable, Autonomous, Urban Reconnaissance Robot", *Robotics and Autonomous Systems,* Vol. 40, Issues 2-3, pp. 163-172, 2002.

[6] D. O'Halloran, A. Wolf and H. Choset, "Design of a High-impact Survivable Robot," *Mechanism and Machine Theory,* Vol. 40, Issue 12, pp. 1345-1366, 2005.

[7] T. Iwamoto and H. Yamamoto, "Mechanical Design of Variable Configuration Tracked Vehicle," *Journal of Mechanical Design,* Vol. 112, Issue 3, pp. 289-294, 1990.

[8]http://www.bluebotics.com/solutions/Shrimp/specification.php

[9] K. Schilling and C. Jungius, "Mobile Robots for Planetary Exploration," *Control Engineering Practice,* Vol. 4, Issue 4, pp. 513-524, 1996.

[10] H. B. Brown, J. M. Vande Weghe, C. A. Bererton, and P. K. Khosla, "Millibot Trains for Enhanced Mobility," *IEEE/ASME Transactions on Mechatronics,* Vol. 7, No. 4, pp. 452-461, 2002.

[11] R. Volpe, "Rocky 7: A next generation mars rover prototype," *Journal of Advanced Robotics*, Vol. 11, No. 4, pp. 341–358, 1997.

[12] J. Suomela, and A. Halme, "Human robot interaction - case WorkPartner," *Proc. IEEE/RSJ Int. Conf. on Intelligent Robots and Systems*, Sendai, Japan, Sep. 28 - Oct. 02, 2004, pp. 3327-3332.

[13] C. Grand, F. Benamar, F. Plumet and P. Bidaud, "Stability and traction optimization of reconfigurable vehicles - Application to a hybrid wheel-legged robot," *The International Journal of Robotics Research*, Vol. 23, No. 10-11, pp. 1041-1058, 2004.

[14] D. Chugo, K. Kawabata, H. Kaetsu, H. Asama and T. Mishima, "Configuration-Based Wheel Control for Step-Climbing Vehicle," *Journal of Robotics and Mechatronics* ,Vol. 19 No. 1 , pp. 52-59, 2007.

[15] F. Barlas, "Design of a Mars Rover Suspension Mechanism," M.Sc. Thesis, Izmir Institute of Technology, Turkey, June 2004.

[16] Y. Kuroda, K. Kondo, K. Nakamura, Y. Kunii and T. Kubota, "Low Power Mobility System for Micro Planetary Rover *Micro5*," *Proc. of the 5th International Symposium on Artificial Intelligence, Robotics and Automation in Space (i-SAIRAS'99)*, pp. 77-82, 1999.